NUKLEONIKA 2017;62(1):17–22
doi: 10.1515/nuka-2017-0003

ORIGINAL PAPER



# A new concept of fusion neutron monitoring for PF-1000 device*

**Slawomir Jednorog, Ewa Laszynska, Barbara Bienkowska, Adam Ziolkowski, Marian Paduch, Kamil Szewczak, Katarzyna Mikszuta, Karol Malinowski, Marcel Bajdel, Pawel Potrykus**

**Abstract.** The power output of plasma experiments and fusion reactors is a crucial parameter. It is determined by neutron yields that are proportional and directly related to the fusion yield. The number of emitted neutrons should be known for safety reasons and for neutron budget management. The PF-1000 is the large plasma facility based on the plasma focus phenomenon. PF-1000 is operating in the Institute of Plasma Physics and Laser Microfusion in Warsaw. Neutron yield changes during subsequent pulses, which is immanent part of this type device and so it must be monitored in terms of neutron emission. The reference diagnostic intended for this purpose is the silver activation counter (SAC) used for many years. Our previous studies demonstrated the applicability of radio-yttrium for neutron yield measurements during the deuterium campaign on the PF-1000 facility. The obtained results were compared with data from silver activation counter and shown linear dependence but with some protuberances in local scale. Correlation between results for both neutron monitors was maintained. But the yttrium monitor registered the fast energy neutron that reached measurement apparatus directly from the plasma pinch. Based on the preliminary experiences, the yttrium monitor was designed to automatically register neutron-induced yttrium activity. The MCNP geometrical model of PF-1000 and yttrium monitor were both used for calculation of the activation coefficient for yttrium. The yttrium monitor has been established as the permanent diagnostic for monitoring fusion reactions in the PF-1000 device.

**Keywords:** dense plasma focus • PF-1000 • neutron diagnostic • activation technique

S. Jednorog, E. Laszynska✉, B. Bienkowska, A. Ziolkowski, M. Paduch, K. Mikszuta, K. Malinowski, P. Potrykus
Institute of Plasma Physics and Laser Microfusion,
23 Hery Str., 01-497 Warsaw, Poland,
Tel.: +48 22 638 1005(45), Fax: +48 22 666 8372,
E-mail: ewa.laszynska@ifpilm.pl

K. Szewczak
Central Laboratory for Radiological Protection,
7 Konwaliowa Str., 03-194 Warsaw, Poland

M. Bajdel
Faculty of Physics, University of Warsaw,
Warsaw, Poland

Received: 25 September 2016
Accepted: 27 October 2016

## Introduction

Neutron yield ($Y_n$) measurement is essential in tokamak and other large plasma experiments [1]. However, small devices such as neutron generators also have to be properly diagnosed in terms of neutron emission rates, energies, and angular distributions [2]. All the time when the neutron yield is in use, it has a meaning of total neutron emission in all directions during the time period, which is characteristic for particular device usually the cycle, pulse, or shot. For the International Thermonuclear Experimental Reactor (ITER) tokamak, $Y_n$ diagnosis and analysis is expected to provide crucial insight on plasmas, as well as information for protection and control [3]. Neutron diagnostics using the Joint European Torus (JET) neutron camera and the neutron time-of-flight spectrometer are used to estimate the fuel density profile in the JET deuterium plasma [4]. This is key to the operation and control of a burning fusion plasma. Neutron flux measurements are also widely used to monitor the reaction rate and fuel burn-up level in nuclear reactors [5]. Neutron

*This paper is based on a presentation given at 13th Kudowa Summer School "Towards Fusion Energy", Kudowa Zdrój, Poland, 13–17 June 2016.

monitors are used to obtain optimum physical parameters in plasma focus devices (PF) for maximum $Y_n$ [6–8]. These procedures enable further analysis of deuteron-deuteron (D-D) pinch reactions in the PF-1000 device and for plasma physics in general.

Currently, $Y_n$ measurements are conducted using fission chambers with the fissile nuclides $^{235}U$, $^{238}U$ and $^{239}Pu$ [1, 3, 9]. The reference is still neutron activation [1, 5], which consists mainly of irradiating an indium sample at well-known geometries, with a known photon detection efficiency, and measuring the neutron-induced activity. Knowledge of the neutron reaction cross section is essential for estimating the neutron flux [4, 10].

All these methods have both limitations and advantages. Indium activation is the reference for deuterium plasma monitoring when 2.45 MeV energy neutrons are produced. Specifically, the indium activation is $^{115}In(n,n')^{115m}In$ reaction. However, niobium will be the reference nuclide for the upcoming Second Experimental Tritium Campaign on the JET tokamak. This is because the nuclear reaction $^{93}Nb(n,2n)^{92m}Nb$ is useful for monitoring 14 MeV neutrons generated during deuterium-tritium (D-T) fusion reactions. Products of both reactions have relatively long lifetimes of 4 hours and 10 days, respectively. Short-lived radionuclides of yttrium, silver, and beryllium are sufficient for monitoring pulsed devices based on PF phenomena [7, 11]. Here, fast neutron yttrium monitoring (FNYM) is used for $Y_n$ measurements at the PF-1000 facilities.

## Materials and methods

### Radiative characteristic of $^{89m}Y$

The $^{89}Y$ nucleus has 50 neutrons and 39 protons and is the only stable isotope of yttrium. In addition, there are at least 20 metastable or excited isomers, including $^{89m}Y$, which is the subject of this work. The following inelastic neutron scattering reaction with yttrium nuclei is suitable for monitoring of 2.45 MeV neutrons produced in a pulsed PF device:

$$n + {}^{89}Y \rightarrow n' + {}^{89m}Y\ (T_{1/2} = 15.663\ s)$$
$$\rightarrow {}^{89}Y + \gamma\ (E_\gamma = 908.96\ keV,\ I_\gamma = 99.16\%)$$

where $T_{1/2}$ is the half-life, $E_\gamma$ is the energy of the gamma ray, and $I_\gamma$ is the intensity of the gamma emission with energy $E_\gamma$. The $^{89m}Y$ also emits X-rays with energies ranging over 1.92–17.013 keV and with intensities of 0.0083–0.295% [12]. The $^{89m}Y$ decay is depicted in Fig. 1.

The half-life $T_{1/2}$ of this isomeric transition (IT) is 15.663 s. Thus, it is possible to use this reaction as the $Y_n$ monitor for pulsed neutron sources. Additionally, it will be ready for reuse after ten $^{89m}Y$ half-lives. Unfortunately, the yttrium monitor is not suitable for fusion devices with repetition times <150 s.

Some nuclear reactions are considered as dosimetry standards in the International Reactor Dosimetry and Fusion File (IRDFF) [13]. The TALYS (i.e., software for the simulation of nuclear reactions) based on Evaluated Nuclear Data Library (TENDL) [14] is also considered a reliable source of nuclear data, however, but not all of those reactions are considered dosimetry standards. The cross section for the $^{89}Y(n,n')^{89m}Y$ is loaded from the TENDL library. It has a threshold for a neutron energy of $E_n$ = 919 keV. The shape of considered cross section is shown in Fig. 2. The cross section is characterized by local maximum and minimum. Neutrons with energies $E_n$ < 1.5 MeV are detected with relatively low efficiency, while high-energy neutrons that come directly from the plasma pinch are detected with high efficiency. Therefore for neutron energy $E_n$ = 2.45 MeV, cross section has a relatively high cross section of 1.36 b. Thus, the newly established monitor could be compared to a collimator that looks selectively through the plasma.

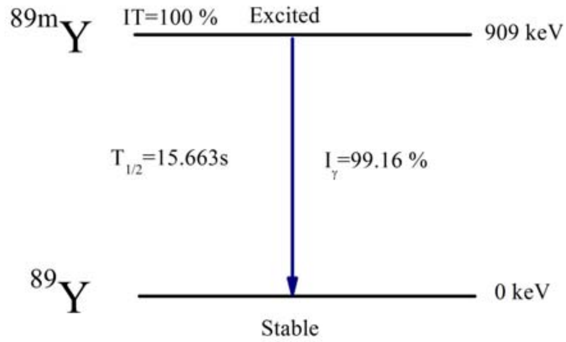


**Fig. 1.** Decay scheme of $^{89m}Y$ metastable state.

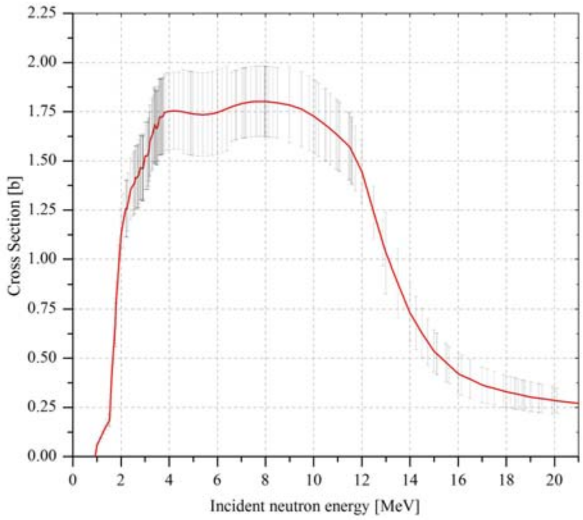


**Fig. 2.** Cross sections for the $^{89}Y(n,n')^{89m}Y$ reaction based on TENDL 2014 nuclear library [14].

### PF-1000

The PF-1000 is based on PF phenomena and is a Mather-type device that works in a pulse mode. It is the largest device of its kind to date. The PF-1000 is equipped with a large battery bank that can be charged up to 40 kV. An energy of 1 MJ is available during high-current discharge. Once the vacuum chamber is filled with deuterium, the high current discharge is induced, and a 2-MA current flows between the electrodes. The current-induced magnetic forces compress the deuterium until it becomes a plasma. Every 15–25 min, a pulse is fired, which produces a dense magnetized plasma. The plasma temperature inside the focus is high enough for deuterium fusion to occur. Additionally, some deuterons are accelerated to energies such that mutual collisions produce intense fluxes of neutrons. Thus, approximately 90–95% of the neutron population comes from the beam/target reaction. The maximum $Y_n$ is $10^{12}$ n/pulse, but is usually $10^{10}$–$10^{11}$ n/pulse. Because $Y_n$ changes during subsequent pulses of the PF-1000 device, it must always be monitored in terms of neutron emission. For a long period of time, the main monitor of $Y_n$ has been the silver activation counter (SAC) [7], but currently, there are also the FNYM and the beryllium neutron activation counter established as the new fashionable neutron diagnostics. Recent reports on plasma formation in the PF-1000 [7, 15, 16] have been focused on designing and testing new plasma diagnostics and materials.

## Monte Carlo N-Particles numerical simulations

Neutron diagnostics calibration requires details of the specific neutron device, such as its geometry and its material composition. In addition, plasma-pinch neutron sources are included as the geometrical input of PF-1000 as well as FNYM (see Figs. 3 and 4) to a Monte Carlo N-Particles (MCNP) transport code. Thus, the derived activation coefficient for yttrium is obtained from numerical simulations of real processes. In practice, we use a reaction rate that is an integral over the product of the reaction cross section and the neutron spectrum at the FNYM. The neutron yield can be calculated by dividing the measured activity of radio-yttrium by the activity resulting from MCNP calculations, which is expressed per one source. The final form of this equation is as follows:

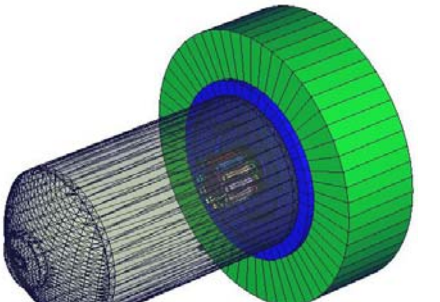

**Fig. 3.** PF-1000 geometrical input for MCNP numerical simulations. The green part is collector, the blue section is isolator, the transparent gray section is vacuum vessel and the multicoloured cylinders are electrodes.

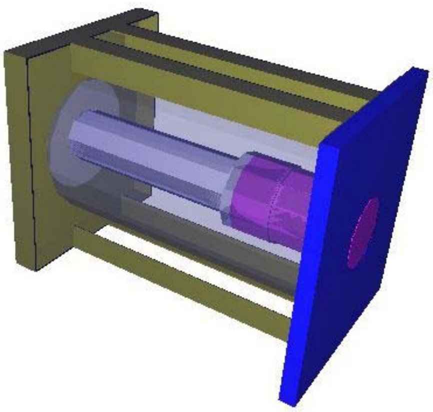

**Fig. 4.** FNYM geometrical input for MCNP numerical simulations. The brown section is frame, the blue part is epoxy glass, the violet section is scintillator, the gray section is photomultiplier, and the transparent gray part is the lead shield.

$$\text{(1)} \qquad Y_n = \frac{\langle \sigma(E)\cdot\varphi(E)\rangle_{ACT}}{\langle \sigma(E)\cdot\varphi(E)\rangle_{MCNP}}$$

where $\sigma(E)$ is the cross section for the particular nuclear reaction as a function of projectile energy, $\varphi(E)$ is the neutron flux at the activation sample as a function of neutron energy, $<\sigma(E)\cdot\varphi(E)>$ is the reaction rate obtained as the integral over the projectile energy $(E_0 - E_{max})$, $E_0$, $E_{max}$ is the minimal and maximal neutron energy reaching the sample, $<\sigma(E)\cdot\varphi(E)>_{ACT}$ is the reaction rate obtained from the yttrium sample activation, and $<\sigma(E)\cdot\varphi(E)>_{MCNP}$ is the reaction rate obtained by MCNP simulations. The neutron source calibration validates the accuracy of the MCNP input.

## Preliminary experiments with yttrium activation

In preliminary tests, an yttrium sample with a mass 80 g and a diameter 60 mm was placed on the PF-1000 vacuum chamber wall, at an angle of 90° to the main axis of the device and on the plane that crosses the center of the plasma focus. The distance from the focus center to the sample surface was 71 cm. After each pulse, the yttrium sample was removed from the device and measured with a high-purity germanium (HPGe) detector. The sample activity was determined on the device discharge moment. An energy efficiency calibration was performed based on the detector numerical characteristics (NCh) and the Laboratory Sourceless Object Calibration Software (LabSOCS®) [17]. The radioactivity of the yttrium sample was linearly dependent on the $Y_n$ measured by the SAC method [7].

## Radio-yttrium monitor of D-D fusion

Based on the preliminary experiments, the $Y_n$ monitor was designed to automatically register neutron-induced yttrium activity. A 3 × 3-in NaI(Tl) scintillator with a photomultiplier was used as the gamma ray detector. The detector was supplied with a generic NCh that enabled an energy-efficiency calibration with LabSOCS.

The activation material used in the FNYM was an yttrium sample with a mass of 114.74 g, a diameter of 80 mm, and a thickness of 5 mm. The detector and activation sample were kept inside the lead-shielded housing (see Fig. 5) mounted directly on the vacuum vessel wall (see Fig. 6). The FNYM and control computer are isolated from electromagnetic

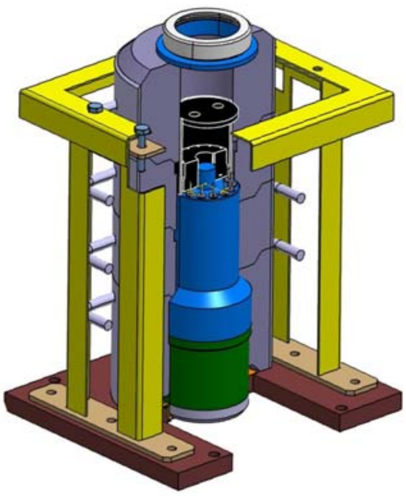

**Fig. 5.** Schematic of the neutron detector in the FNYM. The yellow section is frame, the blue section is the photomultiplier, the green section is the 3 × 3-in NaI(Tl) scintillation detector, and the gray section is lead shielding.

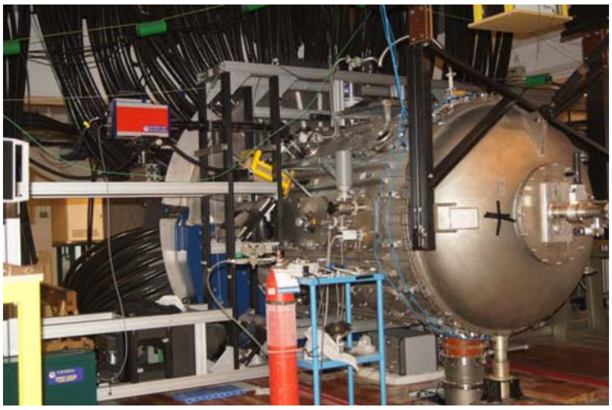

**Fig. 6.** PF-1000 device surrounded by diagnostics. The yellow frame contains the radio-yttrium monitor.

noise generated during the plasma discharge. Because the PF-1000 vessel is neutron-activated [18] between the yttrium and the PF-1000 wall, there is a thin lead plate mounted to absorb gamma radiation from short-lived radionuclides. An externally synched multichannel analyzer (MCA) is used with the TUCAN analyzer, so that after a 200 μs delay following each pulse, the MCA acquires the gamma ray spectrogram.

## Results

The theoretical energy efficiency for the HPGe detection of photons emitted from $^{89m}$Y nuclei during the preliminary experiments was $2.61 \times 10^{-2}$. The results are presented in Fig. 7. There is a linear dependence of the yttrium activation on the neutron emission from the PF-1000 device. However, local discrepancies are sometimes as high as 400%, calculated as the ratio between the local extreme and mean values. The cause of the large errors was the imprecision of the SAC and the radiometry measurements. Fast neutrons generated during D-D reactions have to be slowed down for detection by the SAC, where they undergo radiative capture

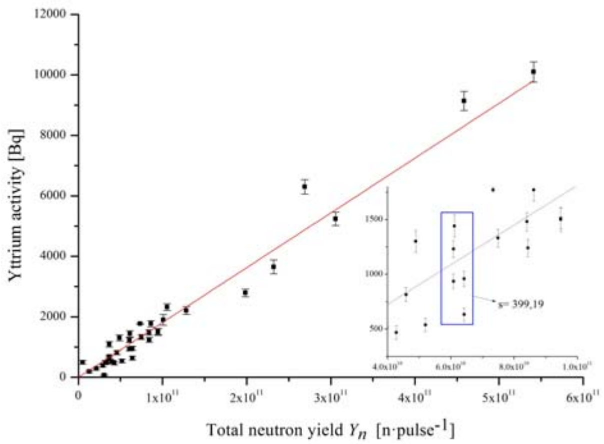


**Fig. 7.** Preliminary results for yttrium sample activation, indicating a linear dependence on total neutron emission. Inset: local perturbations where discrepancies range up to 400%.

(n,γ) reactions. The silver radioactive isotopes emit β-particles, which are registered by a Geiger-Müller counter. In the yttrium monitor, the fast neutrons directly yield gamma rays that are measured by the gamma spectrometer. A disadvantage of the preliminary method was lack of automation and uncertainty in time registration. Therefore, the count rate for the peak of the total energy absorption was lower and the statistics were poor. It should be also noted that the source of neutrons has different shape in each separate discharge of the PF-1000 [16].

It has exhibited an yttrium activation range of 0.7–50 Bq that correspondents to a $Y_n$ range of $9.66 \times 10^8$ up to $1.11 \times 10^{11}$ n/pulse, with uncertainties of 1.39–11.11%.

The absolute full-energy peak efficiency for the gamma quanta ($E_\gamma = 908.96$ keV) emitted after activation from a massive yttrium sample is $7.12 \times 10^{-2}$. This value is higher than that obtained in preliminary experiments with the HPGe detector. However, the NaI(Tl) detector is larger than the HPGe detector, and the yttrium sample is also larger than its equivalent used in the preliminary experiments. In both the preliminary and final methods, the sample was directly on the detector surface. However, the measurement geometry and the sample architecture used for the FNYM yielded registration efficiency.

The activation coefficient calculated by MCNP numerical simulations is $2.46 \times 10^{-29}$. This indicates that one radio-yttrium nucleus is produced by one neutron from one yttrium nucleus in the sample, and thus determines $Y_n$ via yttrium activity. The linear dependence between $Y_n$ for SAC and $Y_n$ for the final model of FNYM was observed. The FNYM has been installed as a permanent neutron diagnostic for the PF-1000 device.

## Uncertainty assessment

The precision of $Y_n$ monitoring by FNYM depends on the MCNP calculation, the measurement of yttrium radioactivity by means of gamma spectrometry, and the efficiency assessment using the generic NCh of the detector. With regard to the MCNP simulations, a geometric model of the PF-1000 device and its surroundings were accurately prepared. However, simplifications are inevitable and their effects on the accuracy are unpredictable. It was also assumed that neutrons are emitted from a point source located in the center of the plasma focus, which should be a sufficient model for neutron activation calculations. The neutron source is located 71 cm from the activation sample. The real mechanism of neutron generation and emission is complex and not thoroughly understood. The number of simulated histories for each neutron source was $2 \times 10^8$. Therefore, the estimated relative errors for the MCNP results are usually below 1%.

With regard to gamma spectrometry, the accuracy of time measurement is very high (±0.01 s), and the error can be neglected. The uncertainty of the radiometric measurements strictly depends on number of registered impulses and varied between 1.39% and 11.11%.

The manufacturer of the NaI(Tl) detector [17] asserted that the generic NCh has an uncertainty of efficiency prediction for gamma quanta ($E_\gamma$ = 908.96 keV) registration of 4%, while our present and previous studies [18] indicate much larger errors. The comparison of the calibration source with the theoretical energy efficiency calibration indicated differences of 45%. So far, the LabSOCS software is one of methods that can provide researchers with gamma ray detection efficiencies for metallic sample geometries. Thus, the total uncertainty is in the range of 15% for the asserted NCh; otherwise, it is up to 50%. The total uncertainty is lower for high-efficiency pulses because of better of radiometry counting statistics.

## Conclusions

During many experiments at the PF-1000 facilities, it was shown that yttrium activation had a significant potential for monitoring emitted neutrons during pulsed D-D experiments. Thus, a fast neutron yttrium monitor was designed for permanent monitoring of neutron emission yields. High-efficiency gamma spectrometry of yttrium activation reports total neutron yield with a sensitivity of at least $9.9 \times 10^8$ n/pulse, with an uncertainty of 11%. The total uncertainty of the system is 15%, while the required uncertainty of the last JET tokamak calibration was 10% [1]. The main uncertainty in accuracy is from the efficiency assessment based on the generic NCh of the detector, which was provided by the manufacturer. For high-efficiency pulses, the total uncertainty is lower because of the higher induced yttrium activity. For $Y_n$ monitoring of D-D experiments on the PF-1000 device, 15% uncertainty is an acceptable value. Higher uncertainties would limit FNYM applications for materials research at the PF-1000 facility. The final results for the FNYM must be confronted with the neutron radial asymmetry for the PF-1000 plasma focus device [16] and reported as separate issue.

**Acknowledgments.** This work was partly supported by the IAEA CRP RC-16956 and RC-17165 grants, as well by the Polish Ministry of Science and Higher Education within the framework of the financial resources in the year 2016 allocated for the realization of the international co-financed projects.

The 13th edition of the Kudowa Summer School "Towards Fusion Energy", held in Kudowa Zdrój, Poland on 13–17 June 2016, was supported by the Polish Physical Society as well as the Polish Ministry of Science and Higher Education.

## References

1. Syme, D. B., Popovichev, S., Conroy, S., Lengar, I., Snoj, L., Sowden, C., Giacomelli, L., Hermon, G., Allan, P., Macheta, P., Plummer, D., Stephens, J., Batistoni, P., Prokopowicz, R., Jednorog, S., Abhangi, M. R., Makwana, R., & JET EFDA. (2014). Fusion yield measurements on JET and their calibration. *Fusion Eng. Des.*, *89*(11), 2766–2775.
2. Laszynska, E., Jednorog, S., Ziolkowski, A., Gierlik, M., & Rzadkiewicz, J. (2015). Determination of the emission rate for the 14 MeV neutron generator with the use of radio-yttrium. *Nukleonika*, *60*(2), 319–322. DOI: 10.1515/nuka-2015-0040.
3. Bertalot, L., Barnsley, R., Direz, M. F., Drevon, J. M., Encheva, A., Jakhar, S., Kashchuk, Y., Patel, K. M., Arumugam, A. P., Udintsev, V., Walker, C., & Walsh, M. (2012). Fusion neutron diagnostics on ITER tokamak. *J. Instrum.*, *7*, 1–18. DOI: 10.1088/1748-0221/7/04/C04012.
4. Eriksson, J., Castegnetti, G., Conroy, S., Ericsson, G., Giacomelli, L., Hellesen, C., & JET-EFDA contributors. (2014). Deuterium density profile determination at JET using a neutron camera and a neutron spectrometer. *Rev. Sci. Instrum.*, *85*(11), 11E106. DOI: 10.1063/1.4889907.
5. Borio di Tigliole, A., Cammi, A., Chiesa, D., Clemenza, M., Manera, S., Nastasi, M., Pattavina, L., Ponciroli, R., Pozzi, S., Prata, M., Previtali, E., Salvini, A., & Sisti, M. (2014). TRIGA reactor absolute neutron flux measurement using activated isotopes. *Prog. Nucl. Energy*, *70*, 249–255. DOI: 10.1016/j.pnucene.2013.10.001.
6. Ellsworth, J. L., Falabella, S., Schmidt, A., & Tang, V. (2014). Ion beam and neutron output from a sub-kilo joule Dense Plasma Focus. *AIP Conf. Proc.*, *1639*(1), 27. http://doi.org/10.1063.1.4904769.
7. Jednorog, S., Szydlowski, A., Bienkowska, B., & Prokopowicz, R. (2014). The application of selected radionuclides for monitoring of the D-D reactions produced by dense plasma-focus device. *J. Radioanal. Nucl. Chem.*, *301*(1), 23–31. DOI: 10.1007/s10967-014-3131-0.
8. Ong, S. T., Chaudhary, K., Ali, J., & Lee, S. (2014). Numerical experiments on neutron yield and soft x-ray study of a ~100 kJ plasma focus using the current profile fitting technique. *Plasma Phys. Control. Fusion*, *56*(7), 075001. DOI: 10.1088/0741-3335/56/7/075001.
9. Bhatia, C., Fallin, B., Gooden, M. E., Howell, C. R., Kelley, J. H., Tornow, W., Arnold, C. W., Bond, E. M., Bredeweg, T. A., Fowler, M. M., Moody, W. A., Rundberg, R. S., Rusev, G., Vieira, D. J., Wilhelmy, J. B., Becker, J. A., Macri, R., Ryan, C., Sheets, S. A., Stoyer, M. A., & Tonchev, A. P. (2014). Dual-fission chamber

and neutron beam characterization for fission product yield measurements using monoenergetic neutrons. *Nucl. Instrum. Methods Phys. Res. Sect. A-Accel. Spectrom. Detect. Assoc. Equip*., *757*, 7–19. DOI: 10.1016/j.nima.2014.03.022.

10. Waugh, C. J., Rosenberg, M. J., Zylstra, A. B., Frenje, J. A., Séguin, F. H., Petrasso, R. D., Glebov, V. Y., Sangster, T. C., & Stoeckl, C. (2015). A method for in situ absolute DD yield calibration of neutron time-of-flight detectors on OMEGA using CR-39-based proton detectors. *Rev. Sci. Instrum*., *86*(5), 053506. DOI: 10.1063/1.4919290.
11. Roshan, M. V., Springham, S. V., Rawat, R. S., Lee, P., & Krishnan, M. (2010). Absolute measurements of fast neutrons using yttrium. *Rev. Sci. Instrum*., *81*(8), 083506. DOI: 10.1063/1.3478020.
12. National Nuclear Data Center, Brookhaven National Laboratory, based on ENSDF and the Nuclear Wallet Cards. (2016, June). *Decay radiation search*. Retrieved June 10, 2016, from http://www.nndc.bnl.gov/nudat2/indx_dec.jsp.
13. Capote, R., Zolotarev, K. I., Pronyaev, V. G., Trkov, A., Zsolnay, E. M., & Nolthenius, H. K. (2014, October). *International Reactor Dosimetry and Fusion File*. Retrieved June 10, 2016, from https://www-nds.iaea.org/IRDFF/.
14. Koning, A. J., Rochman, D., van der Marck, S. C., Kopecky, J., Sublet, J. Ch., Pomp, S., Sjostrand, H., Forrest, R., Bauge, E., Henriksson, H., Cabellos, O., Goriely, S., Leppanen, J., Leeb, H., Plompen, A., Mills, R., & Hilaire, S. (2015, July). *TENDL-2014: TALYS-based evaluated nuclear data library*. Retrieved June 10, 2016, from ftp://ftp.nrg.eu/pub/www/talys/tendl2014.
15. Jednorog, S., Szydlowski, A., Scholz, M., Paduch, M., & Bienkowska, B. (2012). Preliminary determination of angular distribution of neutrons emitted from PF-1000 facility by indium activation. *Nukleonika*, *57*(4), 563–568.
16. Jednorog, S., Paduch, M., Szewczak, K., & Laszynska, E. (2015). Radioindium and determination of neutron radial asymmetry for the PF-1000 plasma focus device. *J. Radioanal. Nucl. Chem*., *303*(1), 941–947. DOI: 10.1007/s10967-014-3444-z.
17. CANBERRA. (2016). *Technical Advantages of ISOCS™/LabSOCS™*. Retrieved June 10, 2016, from http://www.canberra.com/literature/isocs/application_notes/ISOCS-LabSOCS-App-Note-C39530.pdf.
18. Jednorog, S., Polkowska-Motrenko, H., Szewczak, K., Bienkowska, B., Paduch, M., Prokopowicz, R., Ciupek, K., Chajduk, E., Samczynski, Z., Krajewski, P., & Laszynska, E. (2014). Neutron activation of PF-1000 device parts during long-term fusion research. *J. Radioanal. Nucl. Chem*., *303*(1), 1009–1014. DOI: 10.1007/s10967-014-3522-2.